Toward economic flood loss characterization via hazard simulation

2016 Environ. Res. Lett. 11 084006

(http://iopscience.iop.org/1748-9326/11/8/084006)

Environmental Research Letters

LETTER

Toward economic flood loss characterization via hazard simulation

Jeffrey Czajkowski[1,2], **Luciana K Cunha**[2,3], **Erwann Michel-Kerjan**[1] **and James A Smith**[2,3]

[1] Wharton Risk Management and Decision Processes Center, University of Pennsylvania, 3730 Walnut Street, Philadelphia, PA 19104, USA
[2] Willis Research Network, 51 Lime Street, London, EC3M 7DQ, UK
[3] Department of Civil and Environmental Engineering, Princeton University, E413 Engineering Quad, Princeton, NJ 08544, USA

E-mail: jczaj@wharton.upenn.edu

Keywords: tropical cylcone inland flood, simulated streamflow, insured losses, Delaware River Basin, ungauged flood basin

Supplementary material for this article is available online

OPEN ACCESS

RECEIVED
27 April 2015

REVISED
28 April 2016

ACCEPTED FOR PUBLICATION
7 July 2016

PUBLISHED
4 August 2016

Abstract

Among all natural disasters, floods have historically been the primary cause of human and economic losses around the world. Improving flood risk management requires a multi-scale characterization of the hazard and associated losses—the flood loss footprint. But this is typically not available in a precise and timely manner, yet. To overcome this challenge, we propose a novel and multidisciplinary approach which relies on a computationally efficient hydrological model that *simulate*s streamflow for scales ranging from small creeks to large rivers. We adopt a normalized index, the flood peak ratio (FPR), to characterize flood magnitude across multiple spatial scales. The simulated FPR is then shown to be a key statistical driver for associated economic flood losses represented by the number of insurance claims. Importantly, because it is based on a simulation procedure that utilizes generally readily available physically-based data, our flood simulation approach has the potential to be broadly utilized, even for ungauged and poorly gauged basins, thus providing the necessary information for public and private sector actors to effectively reduce flood losses and save lives.

1. Introduction

Of all natural disasters, floods are the most costly [1] and have affected the most people [2]. Losses from worldwide flood events nearly doubled in the 10 years from 2000 to 2009 compared with the prior decade. [52] This trend shows no sign of abating and most countries are exposed to flood hazard, making flood mitigation a universal challenge. Recent large-scale riverine flood events, on which this article focuses, in countries as diverse as Australia (in 2010), China (in 2010 and 2013), Germany (in 2013), Morocco (in 2010), Thailand (in 2011), the UK (in 2012 and 2014) and the US (2011, 2012) demonstrate the urgency to improve preparedness of exposed areas. Effective flood risk management activities—risk reduction, emergency response, recovery—require an accurate and timely characterization of the hazard and its possible consequence (losses) at a given location and for the entire affected region [3]; that is, the *flood loss footprint*. Current significant annual economic damage and human losses caused by riverine floods, combined with projected increases in flood intensity and frequency due to climate change and land cover change [4, 5, 46], highlights the need for such information. However, methods that are able to accurately simulate or observe flood magnitudes over large areas, across multiple spatial scales, and in a timely manner are typically unavailable. Timely here refers to a near real time evaluation of the event (during, and after) with sufficient lead-time for response. Lead-time can be improved by including weather observations and forecasts, and by adopting computationally efficient models that provide results in the matter of seconds.

Ideally, floods would be characterized by detailed maps of inundated areas, depths and duration. Even though detailed hydraulic models have improved in recent years, they still have significant limitations for operational use over large areas with spatial resolution similar to the one applied in this work (unit catchment area on the order of 1 km^2). Limitations include high implementation cost, excessive computational time, and large data requirements [6–9,47–49]. The most efficient hydraulic models can be applied globally if

relatively coarse calculation units are defined (unit catchment area on the order of 500 km^2) [8]. The direct use of only rainfall data to predict flood loss is often not satisfactory because this method neglects the critical land surface processes and built environment that control floods. Dense stream-gauging networks are useful to characterize floods, however there are few settings from a global perspective with adequate gauging density for flood hazard assessment [10–13].

2. Novelty and value of the proposed approach

To overcome these issues, we propose a novel and interdisciplinary methodology that links flood hazard (here represented by the normalized spatial characterization of flood intensity via hydrologic simulation) to flood impacts (here represented by the number of insured flood claims incurred), and allows us to better understand relationships between them. We introduce a computationally efficient multi-scale hydrological model, and a normalized flood index—the flood peak ratio (FPR)—to spatially characterize flood intensity (see Small *et al* [23] for model performance). The FPR relates the intensity of the flood event with the intensity of events that have happened in the past, and more importantly provides a suitable metric for a multi-scale approach to evaluate flood hazard. With a spatially explicit characterization of flood intensity via hydrologic simulation, we are able to investigate the relationship between the simulated flood hazard and the actual insured flood claims, again as proxy for flood impact. As a similarly constructed FPR based on data-driven streamflow has been successfully applied to characterize flood event [35, 36] and flood claim losses [11] over large regions, we utilize this method for validation purposes of our simulated FPR approach. Ultimately, both FPR methods present advantages and limitations and we expect both to be identified as key drivers of incurred flood losses (and as we do find) in our geographical area of study given its dense stream gauging network. But unfortunately, many flood-prone geographical areas in the U.S. and around the world do not have such a dense stream gauge network in place. Thus, the significant contribution of our proposed hydrologic simulation-based methodology is that it has the potential to be applied to many regions given its reliable and computationally efficient way to spatially characterize the flood hazard and the corresponding relationship to flood claim losses as we demonstrate here.

Of course, as in any model application, the accuracy of the results depends on the accuracy and resolution of the key input data or suitable proxies. Note that the necessary physical and hydro-meteorological data is usually available worldwide [14–16], even though the quality of such datasets and their applicability on this methodology are yet to be tested and will be the subject of future work. For example, radar rainfall datasets are not available in many countries. In this case, precipitation datasets provided by rain gauge or remote sensing, which present larger errors, and coarse spatial and temporal resolution, would have to be used. Similarly, insured flood claim data can be difficult to obtain in parts of the world [51], but the statistical relationships developed here between simulated flood hazard and insured flood claims could be used to generate a proxy of direct economic damage and hence begin to outline the economic flood loss footprint. Nevertheless, the methodology presented in this study is especially valuable for the regions for which almost no flood hazard data is available and flood hazard and loss is rarely quantified. If in-place prior to the occurrence of the flood, achieving an accurate and timely characterization of the economic flood loss footprint should be possible. This new capacity can be of high value to a number of public and private sector stakeholders dealing with flood disaster preparedness and loss indemnification (e.g., emergency services, relief agencies, insurers) in low- and high-income countries alike because it is easily and quickly computed.

3. Methods for the local characterization of flooding

As a proof of concept, we apply our methodology to the Delaware River Basin (DRB), on the east coast in the United States, which has a drainage area of 17 560 km^2 at Trenton, New Jersey (NJ) and an exceptionally dense stream gauging network of 72 sites. This allows us to validate the proposed simulated FPR methodology at a fairly granular level using a data-driven FPR for comparative purposes. Moreover, the DRB experiences frequent and intense riverine flooding [17]. Figure 1 shows the location of the DRB in relation to the states of New York (NY), Pennsylvania (PA), and NJ.

While the main channel of the Delaware River is un-dammed, 38 major dams (15 m tall and with storage capacity of at least 6200 000 m^3 or of any height with a storage capacity of 31 000 000 m^3) control the flow of the Delaware River tributaries [18]. A highly controlled environment imposes difficulties for flood simulation, inasmuch as an accurate simulation of the impact of dams on floods requires precise information about the dams' location, surface areas, volumes, operating purposes and rules, information which is usually not readily available. Moreover, dam operations during extreme floods are usually defined in real time by multiple stakeholders, and do not follow static operation rules. We address this issue by applying a simple model to simulate the hydraulic effects of reservoirs. In our model, as in reality, reservoirs act by delaying the flow. The delay rate is defined by two factors: type of reservoir (controlled or not controlled) and the purpose of the reservoir (e.g., water supply,

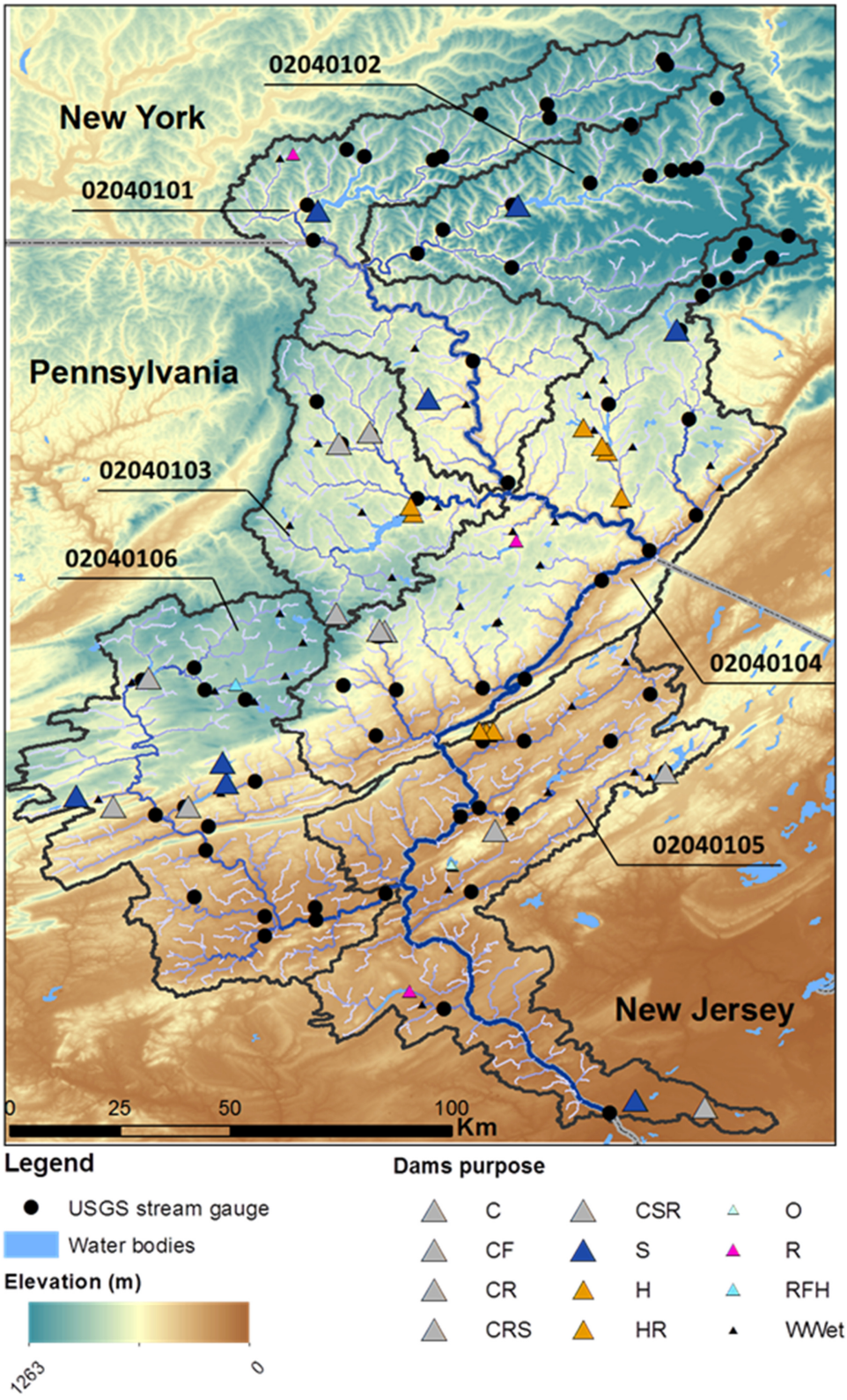

Figure 1. Map of the DRB showing the USGS hydrological units (HUC08) boundaries, the river network, and the location of the USGS streamflow gauges and reservoirs. The reservoirs' purposes are defined as: C: flood control and storm water management, S: water supply, H: hydroelectric, R: recreation, F: fish and wildlife pond, and O: other. WWet refers to reservoirs identified in the water bodies and wetlands database.

flood control). For example, flood control reservoirs have a larger delay rate than water supply, or recreational reservoirs. Even though the model does not exactly replicate reservoirs' outflow hydrographs, it replicates the reservoir effect of delaying and attenuating streamflow.

We characterize the DRB flood hazard through observed *and* simulated streamflow data. Each

method presents advantages and limitations (see M1 for further discussion). Observed streamflow is typically measured at specific discrete points in the river network by stream gauges. To obtain a spatially continuous representation of observed FPR, we first normalize the peak flow of each gauge using its individual 10 year flood peak from the historical record. We then estimate FPR for each link in the river network by interpolating the 72 observed values using the inverse distance weighted approach. This method has been applied by Villarini and Smith [19] to estimate peak flow over the eastern US for major floods [53]. Flood hazard quantification using stream gauging data is sensitive to the density of the network, the spatial variability of the flood event, the interpolation method used, and the number of flow control structures in the basin that introduce unnatural flow alteration.

The sparse nature of stream gauging networks in many settings, however, limits the utility of data-driven approaches to characterize the spatial extent of flooding. The main advantage of a hydrologic simulation approach is that it can be applied in sparse stream-gauge settings. Furthermore, it takes into consideration the river network structure's role in shaping the spatial pattern of flooding. While many distributed hydrological models represent a region by dividing it into a number of regular spatial elements (see Kampf and Burges [20] for a list of models), a watershed is made up of hillslopes, where rainfall runoff transformation occurs, and the river network, that transports the runoff through the drainage basin. Our simulated streamflow methodology discretizes the landscape into these natural elements (hillslopes and river network links) and solves the mass conservation equations for each [21]. With this natural discretization of the terrain, we obtain a more accurate representation of the river network, which is an essential component of a flood simulation model [22]. This model conceptualization allows us to obtain a spatially explicit characterization of floods; hydrographs and peak flow are simulated across multiple scales for each link of the river network in a computationally efficient way [23].

We simulate streamflow using CUENCAS, a spatially explicit physically based hydrological model. Prior flood research using CUENCAS has been presented by Mantilla and Gupta [24], Mandapaka *et al* [25]; Cunha *et al* [5]; Cunha *et al* [26], Seo *et al* [27], Ayalew *et al* [28], Ayalew *et al* [29]. Even though other hydrological models that simulate floods are available, we chose CUENCAS due to its computational efficiency, valid and detailed representation of the river network, simplified parameters estimation based on measurable physical properties, and its ability to simulate floods across a large range of scales (from hillslope to large watersheds). These aspects will be further discussed throughout this paper.

In CUENCAS, the terrain is discretized into hillslope and link that allows the simulation of flood processes close to the scale they occur naturally. Hillslopes provide a more natural terrain discretization than the ad-hoc square grid, triangular, or variable area sub-watershed discretization usually applied in hydrological modeling. This valid representation of the terrain increases our ability to select parameters based on measurable physical properties of the watershed that correctly represent the patterns of runoff generation of each hillslope (see Cunha [33] for details on how parameters can be estimated). The datasets required to implement the model include: (1) digital elevation model for the river network extraction and for the estimation of hydraulic geometry parameters; (2) rainfall as hydrometeorological forcing, (3) land cover, and soil datasets for landscape characterization; and (4) initial soil moisture conditions. These datasets are available through remote sensing or have the potential to be in a near future. These datasets are also available through hydrological reanalyzes [54, 55].

For the DRB model implementation we used 4 km $\times$ 4 km, hourly Stage IV rainfall maps [30], climatological potential evapotranspiration values provided by the MOD16 product [31], topographic characterization provided by the 30 m $\times$ 30 m National Elevation Dataset, soil parameters provided by the 10 m $\times$ 10 m Gridded Soil Survey Geographic (gSSURGO) [32], and hydraulic geometry parameters estimated based on USGS hydraulic measurements (as described by Cunha [33]).

To normalize streamflow with respect to basin scale, and to allow the spatial visualization of flood intensity, we utilize the normalized FPR approach [19]. For each gauge, the FPR is the event flood peak divided by the 10 year flood peak flow value from the historical record. We use the 10 year flood peak since we believe this value can be accurately estimated using relatively short time series (20–30 years). When historical data is not available, this value can be estimated using regionalization [22, 34]. FPRs larger than 1 indicate a flood event with return period larger than 10 years. The FPR based on observed streamflow has been successfully applied to characterize flood event data [35, 36] and flood losses [11] over large regions. A required step to apply this methodology is to estimate regional values for the 10 year peak flow (see M2 for details). To provide a direct link between FPR and flood severity, we followed the methodology employed by Villarini *et al* [37] and estimate the FPRs that correspond to each of the US National Weather Service (NWS) flood categories—action, minor, moderate, and major flooding[4]. In supplementary material figure 1 we present box plots with FPR values for each NWS flood category for sites in the DRB. FPRs lower than 0.51 correspond to 'action'; FPRs greater than 0.51 and less than or equal to 0.78 correspond to 'minor flood'; FPRs greater than 0.78 and less than or

[4] For further description of these categories see http://crh.noaa.gov/arx/?n=flooddefinitions.

equal to 1.08 correspond to 'moderate flood'; and FPRs greater than 1.08 correspond to 'major flood'.

4. Flood hazard simulation and validation from four major events

The dense stream-gauge network of the DRB allows us to assess our simulated peak flow methodology by comparing data-driven and simulated hydrographs, as well as peak flows for the locations for which streamflow data are available. To validate our approach we investigate four different recent (2004, 2005, 2006 and 2011) extreme flood events in the DRB. Smith *et al* [38] presented a detailed description of the Delaware River flood hydrology and hydrometeorology and showed that floods in the Delaware River are produced by a diverse collection of flood-generating mechanisms. The 2004 and 2011 events were caused by extreme rainfall from hurricanes Ivan and Irene, respectively. The 2005 event was caused by a winter–spring extratropical system that combined snowmelt, saturated soils, and heavy rainfall over a period of approximately twenty-four hours. The 2006 flood was the product of a series of mesoscale convective systems that were associated with a trough-ridge system over the eastern US.

Even in a complex drainage basin, with pronounced heterogeneities in rainfall due to orographic precipitation mechanisms, the comparison of simulated and data-driven discharge resulted in high correlation coefficients for almost all gauges (see supplementary material figure 2); the model provides better streamflow estimates than the event average (Nash–Sutcliffe coefficient of efficiency larger than 0) for 72%, 75%, 90%, and 81% of the active gauges for the 2004, 2005, 2006, and 2011 events.

We also present a comparison between simulated and data-driven peak flow scaling (supplementary material figure 3). For all the events, we observe large peak flow variability at small to medium scales (up to approximately 1000 km^2). This variability arises from spatially and temporally variable rainfall, initial soil conditions, runoff generation processes, and travel time dynamics in the channel links. The small-scale variability of peak flow gives raises to spatial scaling (power law) as drainage area increases. It is interesting to note that even in the presence of multiple man-made structures that modify the natural flow, peak flow scaling still holds. The model successfully simulates peak flow scaling patterns. The model underperformed for sites located immediately downstream from reservoirs since we adopted a simplified model to estimate reservoir outflow. However, the effect of the reservoirs decreases as basin scale increases and the model accurately simulates flow across multiple scales (see supplementary material figure 4).

In figure 2 we present maps of data-driven and simulated FPR for the 2004 event overlaid by census tracts that presented at least one flood claim for this flood event (to be detailed in section 5). Maps for the remaining events (2005, 2006, and 2011) are shown in supplementary material figures 5–7. Both methods present advantages and disadvantages. The weaknesses of the data-driven approach is the high sensitivity to gauge density and inability to account for river network flooding. This flaw is visible in the map where areas of influence around the stream gauging station can be identified even with the dense stream gauging network of the Delaware River. The FPR approach is sensitive to data and model uncertainties. The maps in figure 2 present significant differences between data-driven and simulated FPR. Due to limitations in both methods, no method is necessarily better than the other. In areas with high gauge density we expect the data-driven method to be better, while the simulated FPR method is expected to be better in areas with poor gauge density.

5. Summary of flood losses from the four major events

The associated loss data are the actual insurance claims incurred for the 2004, 2005, 2006, and 2011 events by the US National Flood Insurance Program (NFIP). In the United States, coverage for flood damage resulting from rising water is explicitly excluded in homeowners' insurance policies, but such coverage has been available since 1968 through the federally managed NFIP. Thus, the NFIP is the primary source of residential flood insurance [39, 40]. We have access to its entire portfolio from 2000 to 2012 as well as individual policy claim data. This allows us to work with a clean dataset on specific economic losses (here direct residential loss) that is verifiable. A claim paid is officially registered by the federal government so we know for sure a loss has occurred. Other economic loss estimates are not necessarily as clean. For example, state level loss estimates may vary widely between states given inclusion or non-inclusion of uninsured losses, losses to public infrastructure, disaster aid expenditures, etc. The fact that insurance is mostly nonexistent in many countries around the world is not important here since the proposed simulation should provide a good proxy, locally, of flood loss (given local characteristics of the house that will have to be taken into account of course).

For each of these four events and resulting flooding, we determine the total number of residential flood claims incurred and the number of NFIP policies-in-force in the DRB at the census tract level (summary of claims and policies by event in supplementary material table 1; and see M3 for further discussion on how claims and policies determined).

On average across all four events, 30% of our DRB census tracts incurred at least one residential flood claim, with 4919 total claims incurred in the DRB across all four events. The total damage (building and contents) for those events was approximately $181

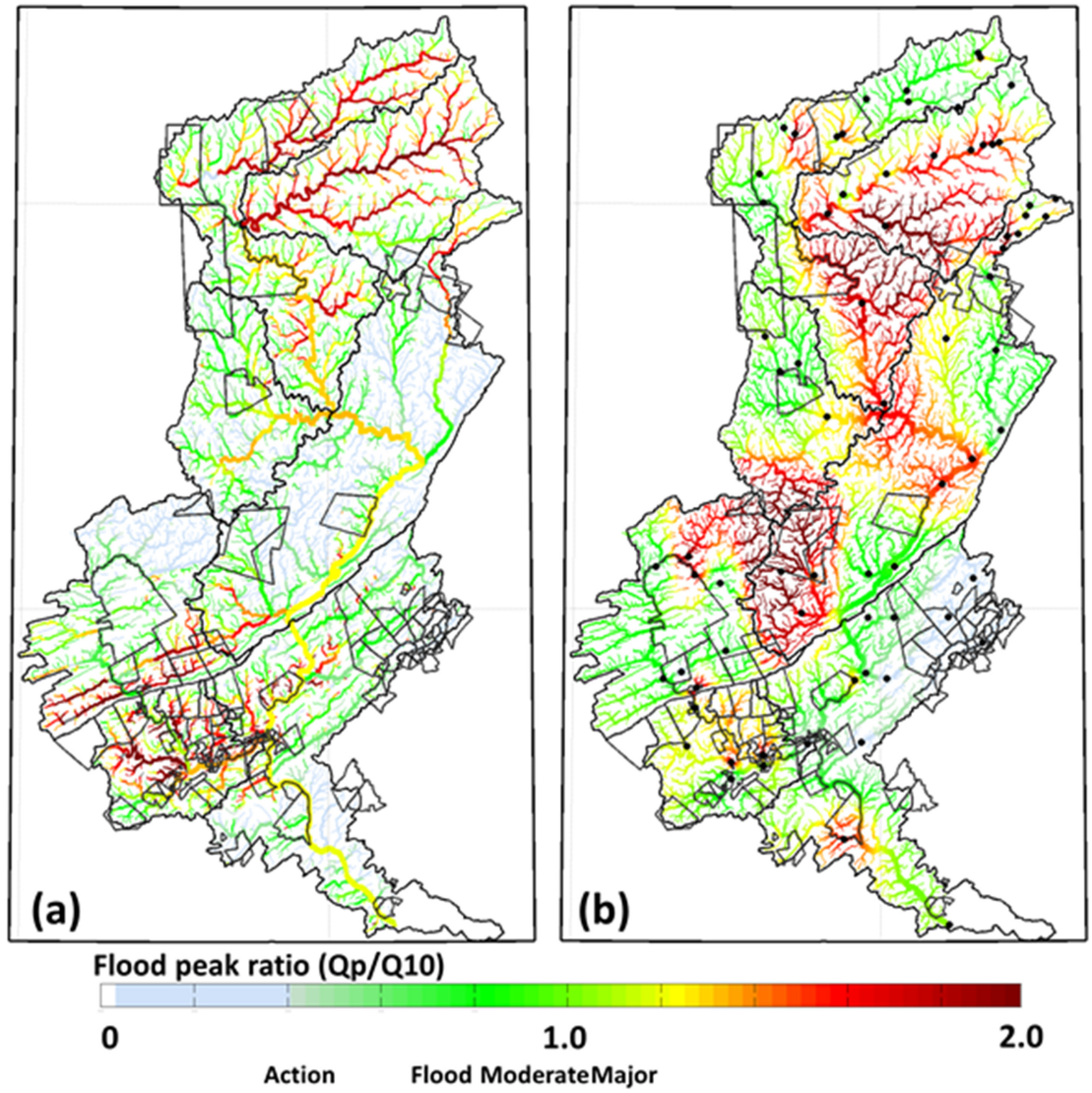

Figure 2. Simulated (a) and data-driven (b) flood peak ratio for the 2004 event. We highlight in black the census tracks that present claims for the event. See supplementary material figures 5–7 for 2005, 2006, and 2011 events.

million (2011 dollars), with a storm-weighted average damage per claim of approximately $36800, which matches well to the mean amount from all NFIP claims across the United States during the period of 1980–2012 of $34500 [50]. These claims were generated from the 5241 NFIP policies-in-force (for the 2004 event) to 9729 NFIP policies-in-force (for 2005, 2006 and 2011 events) in the basin. Given the relatively low flood insurance penetration in the basin (see M3 and supplementary material figure 8 for a map of NFIP policies by census tract), the number of claims and associated losses can be considered a lower-bound estimate of the actual (insured and uninsured) DRB flood losses incurred for these events. But since the vast majority of flood insurance in the US is obtained through the NFIP, our data is a good representation of the number of residential flood insurance claims.

Figure 3 illustrates the straightforward raw data relationship between simulated and observed FPRs (grouped by their associated NWS category) and the number of flood claims. Clearly, FPRs classified as a major flood (>1.08) are associated with the vast majority of the flood claims in the DRB for these studied events. But claims were also incurred for action, minor, and moderate FPRs, and this simple bivariate view of the raw data does not account for any other hazard or exposure characteristics potentially leading to a flood claim. These other potentially relevant aspects will be formally controlled for in the regression analysis below. Importantly, by introducing these controls we will be able to quantify the impact of higher FPR levels on the number of claims incurred, something not able to be determined from figure 3 but important for an accurate and timely characterization of the economic flood loss footprint.

6. Linking local flood hazard to flood loss

In order to determine whether the constructed DRB localized flood hazard (FPR) is in fact a key driver of

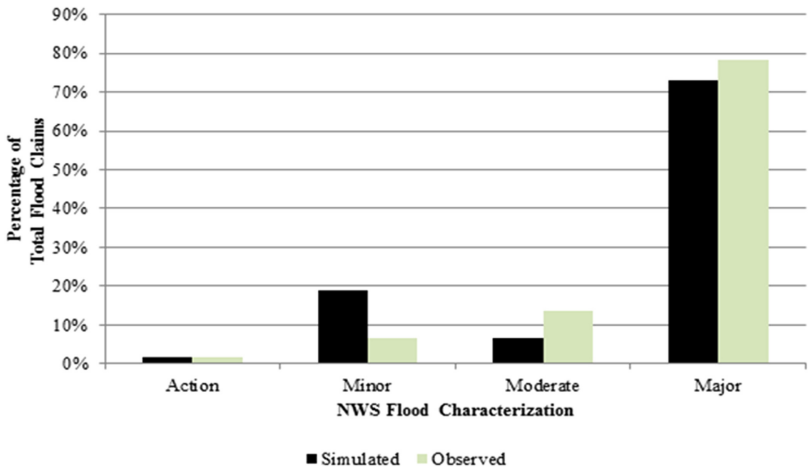

Figure 3. NWS characterized flood peak ratios (simulated and data-driven) and percent of total claims.

residential DRB flood losses (number of residential flood claims) as is expected, and if so, to explicitly quantify by how much residential flood losses change as the flood hazard (FPR) changes, we conduct a multivariate regression analysis on the data from the 2004, 2005, 2006, and 2011 events. The primary purpose of the regression analysis is to statistically identify the causal effect of the flood hazard—simulated and data-driven FPRs—on the number of flood claims incurred in each DRB census tract from each of the four events while also simultaneously controlling for a number of other relevant flood hazard and exposure variables that could causally effect the number of claims incurred as well. We incorporate the FPRs in two distinct ways: first, as the maximum FPR value achieved in each census tract per each event; and second, in order to provide further relative context to these otherwise continuous FPR values, we discretize the maximum FPR into the 'action', 'minor flood', 'moderate flood', and 'major flood'—high water level terminology categories used by the NWS. Although the simulated data-driven approaches are fundamentally different, on average both methods adequately characterize the flood hazard in the DRB as we have shown, thus we expect both FPRs to be key drivers of flood claims.

In addition to the data-driven and simulated FPRs, we added into the regression model controls for other flood hazard characteristics expected to drive the number of flood claims incurred including the size of the census tract ('number pixels' where each pixel is 90 × 90 meters), the density of the river network in the census tract ('percentage river'), and dummy variables along a scale from one to seven that indicate the size of the river. To characterize the size of the river in each tract we use the Horton system of river ordering. We attribute to each tract the largest Horton order. Horton four, the median river size on the seven point scale is the omitted category. The size of the river indicates the type of flood the area is more susceptible to. For example, flash floods are common in small rivers that present fast response to rainfall. Large rivers are more susceptible to floods caused by rainfall events with long duration (see M3). We also control for other relevant exposure factors including the number of housing units and the number of flood insurance policies-in-force in each census tract. All else being equal, as these flood hazard and exposure factors increase, one would expect a larger count of flood insurance claims. It could be that unobserved state-level policies related to land-use, zoning, storm water, etc impact the number of claims incurred per flood event, therefore we control for any unobserved heterogeneity between the three states in the DRB through a fixed effect estimation via state dummy variables (PA, NY, and NJ), with PA the omitted category. For statistical power purposes we pool the data from all four storms; as these are different types of flooding events we also control for any unobserved event-specific fixed effects through event dummy variables (one for each storm; 'extrop', 'cnvctv', 'ivan', 'irene'), with Irene being the omitted category. (See the methods section M3 for a description of the statistical analyses employed. A complete list and description of the variables used in the models is provided in supplementary material table 2.)

Table 1 presents the negative binomial (NB) results where we model the count of claims for the 1435 census tracts with at least one NFIP policy-in-force (full-model results are presented in supplementary material table 3). As we incorporate the FPRs in two distinct ways we present four different models: model 1 utilizes the observed maximum FPR continuous value; model 2 utilizes the simulated maximum FPR continuous value; model 3 utilizes observed maximum FPR discretized NWS classifications; and model 4 utilizes the simulated maximum FPR discretized NWS classifications. All other explanatory variables are the same across all four models. The likelihood ratio chi-squared test for all four models we run indicates that each of the models is

Table 1. Estimated coefficients from count model portion of zero-inflated negative binominal model for 1435 census tracts with at least one NFIP policy-in-force where: model 1 data-driven maximum FPR continuous value; model 2 simulated maximum FPR continuous value; model 3 data-driven maximum FPR discretized NWS classification (major flood is the omitted category); and model 4 simulated maximum FPR discretized NWS classification (major flood is the omitted category). Standard errors are not reported. The log-transformed alpha parameter of the NB distribution captures any overdispersion in the model.

	Negative binomial models for the count of flood claims			
Explanatory variable	Model (1)	Model (2)	Model (3)	Model (4)
Extra tropical 2005	−0.78***	−0.02	−0.67***	−0.09
Convective 2006	−0.19	0.18	−0.15	0.11
Ivan 2004	−0.01	−0.13	−0.11	0.02
NJ	−0.08	−0.26	−0.34*	−0.30*
NY	−0.85***	−0.56***	−0.63***	−0.54**
Housing units	0.00	0.00	0.00	−0.00
NFIP policies	0.03***	0.02***	0.03***	0.02***
Number pixels	−0.00	0.00	0.00	0.00
Percentage river	−0.06***	−0.08***	−0.07***	−0.08***
Horton one	−0.88***	−0.52	−0.93***	−0.43
Horton two	−0.05	0.29	−0.13	0.36
Horton three	0.00	0.25	0.13	0.23
Horton five	−0.30	−0.47**	−0.44**	−0.51**
Horton six	1.21***	0.86***	1.08***	0.98***
Horton seven	1.53***	1.27***	1.42***	1.25***
Data-driven max FPR	0.59***			
Simulated max FPR		0.56***		
Data driven FPR_action			−0.33	
Data driven FPR _minor			−0.42**	
Data driven FPR _moderate			−0.58***	
SimMaxFPR_action				−0.91***
SimMaxFPR_minor				−0.33
SimMaxFPR_moderate				−0.67***
constant	−0.85***	−0.89**	0.09	0.09
Ln alpha	0.77***	0.75***	0.83***	0.76***
N	1435	1435	1435	1435
Log likelihood	−1841.3	−1847.5	−1854.9	−1847.8
LR chi2	541.4	493.0	514.3	492.2
Prob > chi2	0.00	0.00	0.00	0.00

Note. * $p < 0.1$; ** $p < 0.05$; *** $p < 0.01$.

statistically significant at the 1% level. We also see that the number of NFIP policies-in-force and the size of the river (Horton six and seven)—are consistently statistically significant at the 1% level and positive drivers of flood claims for an average census tract in the DRB as expected. Claims increase with the size of the river since floods in larger rivers tend to affect larger areas than floods in small creeks. Therefore, areas closer to a larger river such as the main Delaware stream, are more susceptible to damaging floods. We can explicitly quantify this impact from our estimated Horton six and seven coefficients, where the expected number of claims from an event would increase by a factor of 3.3 and 4.6 respectively as compared to a Horton four river. The major negative driver of flood claims for an average census tract is when the tract is located in NY State—the expected number of claims from an event decreases by 57% in NY State as compared to a census tract located in PA. This is expected since the DRB in NY is comprised mainly of forested areas, with very low population density. From the inflated portion of the NB model (supplementary material table 3) we see that the larger the percentage of river (drainage density) in a tract, the less likely it is to observe zero claims, by 10% for every percentage of river increase. Drainage density is intrinsically linked to the region topography. Likewise, the more NFIP policies-in-force, the less likely it is to observe zero claims.

Models 1 and 3 confirm that the number of claims increases with observed maximum FPR (statistically significant at 1% and 5% levels), as expected. Similar results were found in the relationship between number of claims and observed FPR for 23 states impacted by Hurricane Ivan [11]. What we can further do, though, is quantify this effect. From model 1, if a census tract were to increase its observed maximum FPR by one unit, the expected number of claims from an event would increase by a factor of 1.81 while holding all other variables in the model constant. From model 3, census tracts experiencing FPRs classified as action, minor, or moderate have expected number of claims that are respectively 72%, 66% and 56% of the number

of claims expected for tracts experiencing major FPR while holding all other variables in the model constant[5]. As expected, from the inflated portion of the model (supplementary material table 3), a higher observed FPR value is not a statistically significant driver of a less likely zero-flood claim occurrence.

Most notably, though, from the table 1 results is that simulated FPR coefficient values in models 2 and 4 demonstrate a statistically significant causal effect on the number of flood claims experienced from the four events as expected and as did the data-driven FPR. For both simulated and data-driven flood peak values we see statistical significance at the 1% level for continuous, and categorized FPR (based on NWS flood categories). In an extreme scenario, where no or few streamflow observations are available, the simulated FPR is the only possible applicable method. This result demonstrates the validity of the simulated FPR obtained based on a parsimonious multi-scale hydrological model. The novelty of this work is again in the explicit quantification of these relationships using a method that does not solely rely in observed data. From model 2, if a census tract were to increase its observed maximum FPR by one unit, the expected number of claims from an event would increase by a factor of 1.77 while holding all other variables in the model constant. From model 4, census tracts experiencing FPRs classified as action, minor, or moderate have expected number of claims that are respectively 40%, 71% and 51% of the number of claims expected for tracts experiencing major FPR while holding all other variables in the model constant. Lastly, we see from the inflate portion of models 2 and 4 (supplementary material table 3) that larger simulated FPR values are statistically significant drivers of a lower likelihood of observing a zero-flood claim for an average census tract.

We validate our regression results in two main ways: (1) we apply a *k-fold* cross validation on models (1)–(4) in order to evaluate their ability to fit out-of-sample data (see the methods section M4 for a description of the cross-validation statistical analyses employed); and (2) in supplementary material figure 9 we generate a map of the number of predicted versus actual flood claims using the results from models (1)—observed maximum FPR—and (2)—simulated maximum FPR. The pseudo-*R*-squared statistics generated from *k-fold* cross validation (supplementary material table 4) indicate that zero-inflated negative binomial (ZINB) models (1)–(4) consistently capture about 30% of the variation in out-of-sample test data. The cross-validation goodness-of-fit results are in-line with the full model results, providing further evidence of their validity. Furthermore, in all *k-fold* estimation, the key FPR variables of interest perform as they did in models (1)–(4) in terms of magnitude, sign, and statistical significance.

From supplementary material table 1, the 380 DRB 2010 census tracts utilized for this study incurred a total of 4283 residential flood claims from the 2005, 2006, and 2011 events. Supplementary material figure 9 (left panel) highlights the 61 DRB census tracts (16% of total 380 tracts) that individually incurred at least 10 total claims across these three events (maximum of 336 claims) and together represent 3801 of the total 4283 residential flood claims (89% of total claims). These 61 census tracts are denoted 'DRB high claim tracts'. From the model (1) results utilizing the data-driven maximum FPR in each tract, 56 census tracts are predicted to have 10 or more total claims (middle panel of supplementary material figure 9) across these three events and are denoted 'DRB high claim tracts observed max'. 46 of these model (1) predicted high claim tracts are a match to one of the 61 high claim tracts from the actual NFIP claim data, with census tract matches occurring in all three states of NJ, NY, and PA. Similarly, from the model (2) results utilizing the simulated maximum FPR in each tract, 58 census tracts are predicted to have 10 or more total claims (right panel of supplementary material figure 9) across these three events and are denoted 'DRB high claim tracts simulated max'. 49 of these model (2) predicted high claim tracts are a match to one of the 61 high claim tracts from the actual NFIP claim data, with census tract matches again occurring in all three states of NJ, NY, and PA. Thus, from supplementary material figure 9 middle and right panels we see that the predicted count of claims utilizing the estimated coefficients from table 1 models (1) and (2) respectively, accurately represent these high flood claim census tract areas of the DRB realized from these three events, providing further validity to our estimated models utilizing both data-driven and simulated FPR data.

7. Conclusions and future research

Previous research has shown that observed FPRs can be used to spatially characterize flood events [19, 35, 36] and are key statistical drivers of the number of flood claims incurred for riverine flooding from tropical cyclones (TC) in the eastern US [11]. In this study we again confirm these findings, and more importantly, we propose a methodology that does not solely rely on observed streamflow data. Observed streamflow data are not readily available in satisfactory density for flood hazard characterization in most areas of the world, especially in some of the regions with the highest vulnerability to floods [12, 13]. To demonstrate the sensitivity of estimated flood intensity on gauge density, we present in supplementary material figure 10 observed FPR values for the 2006 flood event based on different number of gauges.

[5] Additionally, a separate estimation not shown using dummy variable for simulatedmax_major = 1, 0 otherwise indicate census tract experiencing a simulated FPR classified as major have exp (.596 3917) = 1.81 times the expected number of claims for tract with value that is less than NWS major flood.

Results presented in this study show that simulated FPR estimated from a physically based hydrological model identifies a causal effect on the number of flood claims in the Delaware River Basin for major flood events, similar to the data-driven FPR obtained from a dense stream-gauging network, which provides a proof of concept across four different storms. We further validate this estimated effect utilizing our model results to predict out-of-sample and observed claims. We believe the proposed simulated FPR method for flood hazard characterization can potentially be applied to many other regions of the world using routinely available remote sensing data sets for digital elevation models [15], rainfall [14], land cover [16], and soil properties [41–43]. Regional flood frequency estimates can be obtained based on empirical and modeling approaches (e.g., Viglione *et al* [44], Guo *et al* [34]). The simulated FPR depends on the accuracy of the input and forcing data. For example, where radar rainfall datasets are not available, precipitation datasets provided by rain gauge or remote sensing would have to be used. Or the statistical relationships developed here between simulated flood hazard and insured flood claims could be used to generate a proxy of the economic flood loss footprint where flood claim data can be difficult to obtain, or where there is no insurance data [51] (local parameters such as construction type and housing cost would have to be considered as well). However, our approach provides a unique, reliable and computationally efficient way to spatially characterize floods in ungauged and/or poorly gauged regions.

Our findings highlight the technological capabilities that can lead to a better integrated risk assessment of extreme riverine floods in a more precise and timely manner. This capacity should be of tremendous value to a number of public and private sector stakeholders dealing with flood disaster preparedness and loss estimation/forecasting and financial indemnification of victims of floods around the world: scientific forecasters, emergency teams, engineers and urban planners, local and national governments as well as residence and building owners and their insurers, when flood insurance is available [45].

References

[1] Miller S, Muir-Wood R and Boissonnade A 2008 An exploration of trends in normalized weather-related catastrophe losses *Climate Extremes and Society* ed H F Diaz and R J Murnane (Cambridge, UK: Cambridge University Press) pp 225–47

[2] Stromberg D 2007 Natural disasters, economic development, and humanitarian aid *J. Econ. Perspect.* **21** 199–222

[3] Van Dyck J and Willems P 2013 Probabilistic flood risk assessment over large geographical regions *Water Resour. Res.* **49** 3330–44

[4] Min S-K, Zhang X, Zwiers F W and Hegerl G C 2011 Human contribution to more-intense precipitation extremes *Nature* **470** 378–81

[5] Cunha L K, Krajewski W F and Mantilla R 2011 A framework for flood risk assessment under nonstationary conditions or in the absence of historical data *J. Flood Risk Manage.* **4** 3–22

[6] Paiva R C D, Collischonn W and Tucci C E M 2011 Large scale hydrologic and hydrodynamic modeling using limited data and a GIS based approach *J. Hydrol.* **406** 170–81

[7] Hodges B R 2013 Challenges in continental river dynamics *Environ. Modelling Softw.* **50** 16–20

[8] Yamazaki D, de Almeida G A M and Bates P D 2013 Improving computational efficiency in global river models by implementing the local inertial flow equation and a vector-based river network map *Water Resour. Res.* **49** 7221–35

[9] Wu H, Adler R F, Tian Y, Huffman G O J, Li H and Wang J 2014 Real-time global flood estimation using satellite-based precipitation and a coupled land surface and routing model *Water Resour. Res.* **50** 2693–717

[10] Perks A, Winkler T and Stewart B 1996 *The Adequacy of Hydrological Networks: a Global Assessment* HWR-52, WMO-740 WMO, Geneva, Switzerland

[11] Czajkowski J, Villarini G, Michel-Kerjan E and Smith J A 2013 Determining tropical cyclone inland flooding loss on a large-scale through a new flood peak ratio-based methodology *Environ. Res. Lett.* **8** 1–7

[12] Beighley E and McCollum J 2013 Assessing global flood hazards: engineering and insurance applications *Presentation at 3rd Int. Workshop on Global Flood Monitoring & Modelling (University of Maryland College Park, MD, USA)*

[13] Dell M, Jones B and Olken B 2013 What do we learn from the weather? The new climate-economy literature *J. Econ. Literature* **52** 740–98

[14] Tapiador F J *et al* 2012 Global precipitation measurement: methods, datasets and applications *Atmos. Res.* **104–105** 70–97

[15] Slater J A, Heady B, Kroenung G, Curtis W, Haase J, Hoegemann D, Shockley C and Tracy K 2011 *Global Assessment of The New ASTER Global Digital Elevation Model: Photogrammetric Engineering and Remote Sensing* vol 77 pp 335–49

[16] Mark A F, Sulla-Menashe D, Tan B, Schneider A, Ramankutty N, Sibley A and Huang X 2010 MODIS Collection 5 global land cover: algorithm refinements and characterization of new datasets *Remote Sens. Environ.* **114** 168–82

[17] Smith J A, Villarini G and Baeck M L 2011 Mixture distributions and the hydroclimatology of extreme rainfall and flooding in the Eastern United States *J. Hydrometeor* **12** 294–309

[18] National Atlas 2009 Major dams of the United States (http://nationalatlas.gov/mld/dams00x.htmlOgden) Ogden F L and Dawdy D R 2003 Peak discharge scaling in small hortonian watershed *J. Hydrol. Eng.* **8** 64–73

[19] Villarini G and Smith J A 2010 Flood peak distributions for the eastern United States *Water Resour. Res.* **46** W06504

[20] Kampf S K and Burges S J 2007 A framework for classifying and comparing distributed hillslope and catchment hydrologic models *Water Resour. Res.* **43** W05423

[21] Gupta V K, Mantilla R, Troutman B M, Dawdy D and Krajewski W F 2010 Generalizing a nonlinear geophysical flood theory to medium-sized river networks *Geophys. Res. Lett.* **37** L11402

[22] Gupta V K and Waymire E 1998 Spatial variability and scale invariance in hydrologic regionalization *Scale Dependence and Scale Invariance in Hydrology* ed G Sposito (Cambridge: Cambridge University Press) pp 88–135

[23] Small S J, Jay L O, Mantilla R, Curtu R, Cunha L K, Fonley M and Krajewski W F 2013 An asynchronous solver for systems of ODEs linked by a directed tree structure *Adv. Water Resour.* **53** 23–32

[24] Mantilla R and Gupta V K 2005 A GIS numerical framework to study the process basis of scaling statistics in river networks *IEEE Geosci. Remote Sensing Lett.* **2** 404–8

[25] Mandapaka P V, Krajewski W F, Mantilla R and Gupta V K 2009 Dissecting the effect of rainfall variability on the statistical structure of peak flows *Adv. Water Resour.* **32** 1508–25

[26] Cunha L K, Mandapaka P V, Krajewski W F, Mantilla R and Bradley A A 2012 Impact of radar-rainfall error structure on estimated flood magnitude across scales: an investigation based on a parsimonious distributed hydrological model *Water Resour. Res.* **48** W10515
[27] Seo B-C, Cunha L K and Krajewski W F 2013 Uncertainty in radar-rainfall composite and its impact on hydrologic prediction for the eastern Iowa flood of 2008 *Water Resour. Res.* **49** 2747–64
[28] Ayalew T B, Krajewski W and Mantilla R 2013 Exploring the effect of reservoir storage on peak discharge frequency *J. Hydrol. Eng.* **18** 1697–708
[29] Ayalew T B, Krajewski W F, Mantilla R and Small S J 2014 Exploring the effects of hillslope-channel link dynamics and excess rainfall properties on the scaling structure of peak-discharge *Adv. Water Resour.* **64** 9–20
[30] Kitzmiller D *et al* 2011 Evolving multisensor precipitation estimation methods: their impacts on flow prediction using a distributed hydrologic model *J. Hydrometeor* **12** 1414–31
[31] Mu Q, Zhao M and Running S W 2011 Improvements to a MODIS global terrestrial evapotranspiration algorithm *Remote Sens. Environ.* **115** 1781–800
[32] Soil Survey Staff, Gridded Soil Survey Geographic (gSSURGO) Database for New Jersey, Pennsylvania, and New York, United States Department of Agriculture, Natural Resources Conservation Service, available online at (http://datagateway.nrcs.usda.gov/.2014)
[33] Cunha L K 2012 Exploring the benefits of satellite remote sensing for flood prediction across scales *PhD Thesis* The University of Iowa, Iowa City, IA
[34] Guo J, Li H-Y, Leung L R, Guo S, Liu P and Sivapalan M 2014 Links between flood frequency and annual water balance behaviors: a basis for similarity and regionalization *Water Resour. Res.* **50** 2
[35] Villarini G, Smith J A, Baeck M L, Marchok T and Vecchi G A 2011 Characterization of rainfall distribution and flooding associated with US landfalling tropical cyclones: analyses of Hurricanes Frances, Ivan, and Jeanne (2004) *J. Geophys. Res.* **116** D23116
[36] Rowe S T and Villarini G 2013 Flooding associated with predecessor rain events over the Midwest United States *Environ. Res. Lett.* **8** 1–5
[37] Villarini G, Goska R, Smith J A and Vecchi G A 2014 North Atlantic tropical cyclones and US flooding *Bull. Am. Meteorol. Soc.* **95** 1381–8
[38] Smith J A, Baeck M L, Villarini G and Krajewski W F 2010 The hydrology and hydrometeorology of flooding in the Delaware River Basin *J. Hydrometeorology* **11** 841–59
[39] Michel-Kerjan E 2010 Catastrophe economics: the national flood insurance program *J. Econ. Perspect.* **24** 165–86
[40] Michel-Kerjan E and Kunreuther H 2011 Redesigning flood insurance *Science* **333** 408–9
[41] Batjes N H 1997 A world dataset of derived soil properties by FAO–UNESCO soil unit for global modelling *Soil Use Manage.* **13** 9–16
[42] Batjes N H 2009 Harmonized soil profile data for applications at global and continental scales: updates to the WISE database *Soil Use Manage.* **25** 124–7
[43] Kerr Y H *et al* 2012 The SMOS soil moisture retrieval algorithm, geoscience and remote sensing *IEEE Trans.* **50** 1384–403
[44] Viglione A, Merz R, Salinas J L and Blöschl G 2013 Flood frequency hydrology: III. A bayesian analysis *Water Resour. Res.* **49** 675–92
[45] Aerts J, Botzen W, Emanuel K, Lin N, de Moel H and Michel-Kerjan E 2014 Evaluating flood resilience strategies for costal megacities *Science* **344** 473–5
[46] Hattermann F F, Huang S, Burghoff O, Willems W, Österle H, Büchner M and Kundzewicz Z 2014 Modelling flood damages under climate change conditions—a case study for Germany *Nat. Hazards Earth Syst. Sci.* **14** 3151–68
[47] Falter D, Dung N V, Vorogushyn S, Schröter K, Hundecha Y, Kreibich H, Apel H, Theisselmann F and Merz B 2016 Continuous, large-scale simulation model for flood risk assessments: proof-of-concept *J. Flood Risk Manage.* **19** 3–21
[48] Falter D, Schröter K, Dung N V, Vorogushyn S, Kreibich H, Hundecha Y, Apel H and Merz B 2015 Spatially coherent flood risk assessment based on long-term continuous simulation with a coupled model chain *J. Hydrol.* **524** 182–93
[49] Winsemius H C, Van Beek L P H, Jongman B, Ward P J and Bouwman A 2013 A framework for global river flood risk assessments *Hydrol. Earth Syst. Sci.* **17** 1871–92
[50] Kousky C and Michel-Kerjan E 2015 Examining flood insurance claims in the United States *J. Risk Insur.* in press (doi:10.1111/jori.12106)
[51] Surminski S and Oramas-Dorta D 2013 Do flood insurance schemes in developing countries provide incentives to reduce physical risks? *Grantham Research Institute on Climate Change and the Environment Working Papers* 119
[52] Zurich Insurance Company 2014 Enhancing community flood resilience: a way forward, Zurich Risk Nexus (http://opim.wharton.upenn.edu/risk/library/zurichfloodresiliencealliance_ResilienceIssueBrief_2014.pdf)
[53] Skøien J, Merz R and Blöschl G 2006 Top-kriging—geostatistics on stream networks *Hydrol. Earth Syst. Sci.* **10** 277–87
[54] Rodell M *et al* 2004 The global land data assimilation system *Bull. Am. Meteorol. Soc.* **85** 381–94
[55] Fan Y, van den Dool H, Lohmann D and Mitchell K 2006 1948–1998 US hydrological reanalysis of the noah land data assimilation system *J. Clim.* **19** 1214–37